

Prediction of solid volume fraction and mean density distribution isograms in slurry flow in a pipe, using ASM model

V.Daei, N.Saghatoleslami

Chemical Engineering Department, Ferdowsi University of Mashhad, (IRAN)

E-mail : slami@um.ac.ir

ABSTRACT

Although many works has been conducted in the field of solid-liquid flow; however, no work has been done on the volume fraction and density distributions, velocity profiles and mean skin friction coefficient distributions in the entrance region of solid-liquid flow. Therefore, in this work a simplified 3-D algebraic slip mixture model (ASM) was adopted for the determination of volume fraction and velocity isograms in slurry flow (i.e., silica sand-water) in a horizontal pipe. In order to obtain this objective, an assumption of fully developed flow was made and the RNG $k-\varepsilon$ model for the turbulent flow with the algebraic slip mixture model was utilised. To solve the flow governing equations and discretize the computation domain, an unstructured (block-structured) with non-uniform grid was chosen using a control volume finite difference method (CVFDM). In order to validate the numerical mean pressure gradients obtained in this study, it was compared with the experimental data available in the literature. The result of this study reveals that there exist a good compatability between the present findings and the experimental data available in the literature. © 2015 Trade Science Inc. - INDIA

KEYWORDS

Algebraic slip mixture;
Control volume finite difference method;
Entrance region;
Fully developed turbulent flow.

INTRODUCTION

Solid-liquid flow in pipelines is a popular mode of transportation in various industries. In general, the solid-liquid flow is divided into three major flow patterns: (1) pseudo-homogeneous flow (or homogeneous flow), in which solid particles are suspended uniformly; (2) heterogeneous and sliding bed flow (or moving bed flow); and (3) saltation and stationary bed flow^[1]. It was founded that when the solid-liquid flow rate is too low to suspend all solid particles, a stationary bed layer at the bottom of the pipe cross-section was observed. Furthermore, the bed layer in the solid-liquid flow was unstable and dangerous during the operation of the pipeline transportation which would probably enhances the

pipe to wear causing the plugging or blockage of the pipeline. Hence, it should be avoided in the design and operation of the pipeline transportation system^[1].

Thompson and co-workers has employd the micro-molecular tagging velocimetry (muMTV) to characterize the hydrodynamic devolping flow in a microtube inlet with a n diameter of 180 μm ^[2]. Orû and Galanis has also examined the inûence of the Lewis number on laminar mixed convective heat and mass transfer in a horizontal tube with uniform heat flux and concentration at the fluid-solid interface^[3]. Al Araby and co-workers presented a numerical study and experimental investigation of single phase combined free and forced convection in the entry region of a horizontal pipe of constant wall temperature with simultaneous develop-

Full Paper

ment of fluid flow velocity and temperature^[4]. Li and co-workers have developed a mathematical model to describe the motion of particles in a current carrying liquid metals flowing through a cylinder pipe^[5]. Coldwell and Shook have determined experimentally the entry length of horizontal slurry pipelines using a pipeline of diameter 50 mm^[6]. Ling and co-workers presented a numerical investigation of double slurry flow in the pipe for the fully developed turbulent flow using Eulerian granular multiphase (EGM) model^[7].

The solid-liquid flow is very complex. In a survey of the open literature on solid-liquid flow investigations including the recent studies conducted by Skudarnov and co-workers, it was found that most of the investigations were made in the laboratories to determine the pressure gradients and critical deposition velocities in solid-liquid flows^[8,9]. Doron and Barnea proposed two-layer and three-layer models of the solid-liquid flow^[1-10] and Wilson and Pugh put forward a dispersive-force modeling in heterogeneous solid-liquid flow^[11]. However, these models were derived based on one-dimensional, single-species, solid-liquid flow; and therefore, they could not determine the density and volume fraction distributions, and velocity profiles of the solid-liquid flow. Nassehi and Khan provided a numerical method for the determination of slip characteristics between the layers of a two-layer slurry flow, but no comparisons of experimental data with numerical results were reported^[12]. In addition, Doron and co-workers have presented numerical and experimental results of slurry flow in horizontal pipes^[13]. Although many works has been conducted in the field of solid-liquid flow; however, no work has been done on the volume fraction and density distributions, velocity profiles and mean skin friction coefficient distributions in the entrance region of solid-liquid flow.

Therefore, in this work a simplified 3-D algebraic slip mixture model was adopted in order to determine the volume fraction and velocity isograms in slurry flow for silica sand-water in a horizontal pipe.

MATHEMATICAL MODELINGS

Governing equations

In this work, the algebraic slip mixture (ASM) model was utilised which could model two-phase flow (i.e., solid-liquid) by solving the momentum equation

and continuity equation for the mixture, the volume fraction equation for the secondary phase and an algebraic expression for the relative velocity^[14]. The continuity equation for the mixture is defined as:

$$\frac{\partial}{\partial t}(\rho_m) + \frac{\partial}{\partial x_i}(\rho_m u_{m,i}) = 0 \quad (1)$$

The momentum equation for the mixture is expressed as:

$$\begin{aligned} & \frac{\partial}{\partial t} \rho_m u_{m,j} + \frac{\partial}{\partial x_i} \rho_m u_{m,i} u_{m,j} \\ &= \frac{\partial p}{\partial x_j} + \frac{\partial}{\partial x_i} \mu_m \left(\frac{\partial u_{m,i}}{\partial x_j} + \frac{\partial u_{m,j}}{\partial x_i} \right) + \rho_m g_i + F_j \\ &+ \frac{\partial}{\partial x_i} \sum_{k=1}^n \alpha_k \rho_k u_{DK,i} u_{DK,j} \end{aligned} \quad (2)$$

where n is the number of phases, F is the body force, α_k is the volume fraction of solids and ρ_m is the mixture density. In Equation 2, μ_m is the viscosity of the mixture and is defined as:

$$\rho_m = \sum_{k=0}^n \alpha_k \rho_k \quad \text{and} \quad \mu_m = \sum_{k=1}^n \alpha_k \mu_k \quad (3)$$

where \vec{u}_m and \vec{u}_{DK} are mass-averaged and drift velocities, respectively and which are expressed as:

$$\vec{u}_m = \frac{\sum_{k=1}^n \alpha_k \rho_k \vec{u}_k}{\rho_m} \quad \text{and} \quad \vec{u}_{DK} = \vec{u}_k - \vec{u}_m \quad (4)$$

The slip velocity is the velocity of the secondary phase (p) relative to the primary phase (q) velocity and is defined as:

$$\vec{v}_{qp} = \vec{u}_p - \vec{u}_q \quad (5)$$

In the above equations, the drift and slip velocity are related by the following expression:

$$\vec{u}_{Dp} = \vec{v}_{qp} - \sum_{i=1}^n \frac{\alpha_i \rho_i}{\rho_m} \vec{v}_{qi} \quad (6)$$

The basic assumption in the algebraic slip mixture model is to prescribe an algebraic relation for the rela-

tive velocity and a local equilibrium between the phases should be reached over short spatial length scales. The slip velocity in the above equation is defined as:

$$\vec{v}_{qp} = \frac{\tau_p}{f_{drag}} \frac{\rho_m - \rho_p}{\rho_p} \vec{a} \quad (7)$$

where \vec{a} is the secondary phase particle's acceleration,

τ_p is the particulate relaxation time, $\tau_p = \frac{\rho_m d_p^2}{18\mu_q}$, and

d_p is the particle diameter. The volume fraction equation for the secondary phase is defined as:

$$\frac{\partial}{\partial t}(\alpha_p \rho_p) + \frac{\partial}{\partial x_i}(\alpha_p \rho_p u_{m,i}) = -\frac{\partial}{\partial x_i}(\alpha_p \rho_p u_{Dp,i}) \quad (8)$$

The algebraic slip mixture model could be applied in both the laminar and turbulent two phase flows. In practice, since the slurry transportation is in the fully developed turbulent flow; in this work, the RNG $k-\varepsilon$ turbulent model was utilised with the algebraic slip mixture model. The turbulent kinetic energy in RNG $k-\varepsilon$ turbulent model is defined as:

$$\begin{aligned} \frac{\partial}{\partial t}(\rho_m k) + \frac{\partial}{\partial x_i}(\rho_m u_{m,i} k) &= \frac{\partial}{\partial x_i} \left[\left(a_k \mu_m \frac{\partial k}{\partial x_i} \right) \right] + \mu_t S_i \\ &+ \beta g_i \frac{\mu_t}{Pr_t} \frac{\partial T}{\partial x_i} - \rho_m \varepsilon \end{aligned} \quad (9)$$

Dissipation rate of the turbulent kinetic energy is expressed as:

$$\begin{aligned} \frac{\partial}{\partial t}(\rho_m \varepsilon) + \frac{\partial}{\partial x_i}(\rho_m u_{m,i} \varepsilon) &= \frac{\partial}{\partial x_i} \left[\left(a_\varepsilon \mu_m \frac{\partial \varepsilon}{\partial x_i} \right) \right] + C_{1\varepsilon} \\ &\times \frac{\varepsilon}{k} \mu_t S^2 - C_{2\varepsilon} \rho_m \frac{\varepsilon^2}{k} - R \end{aligned} \quad (10)$$

Where the coefficients, a_k and a_ε are the inverse effect Prandtl numbers for k and ε , respectively. In Equation 10, β and Pr_t are the coefficients of thermal expansion and turbulent Prandtl number for energy, respectively. For the high-Reynolds numbers, $a_k = a_\varepsilon E^{1.393}$ and $C_{1\varepsilon}$ and $C_{2\varepsilon}$ are 1.42 and 1.68, respectively. In Equation 10, S is the modulus of the mean rate-of-strain tensor (i.e., S_{ij}) and are defined as:

$$S = \sqrt{2S_{ij}S_{ij}} \quad \text{and} \quad S_{ij} = \frac{1}{2} \left(\frac{\partial u_i}{\partial x_j} + \frac{\partial u_j}{\partial x_i} \right) \quad (11)$$

R in Eq. (10) is expressed as:

$$R = \frac{C_\mu \rho_m \eta^3 (1 - \eta/\eta_0)}{1 + \zeta \eta^3} \cdot \frac{\varepsilon^2}{k} \quad (12)$$

where $\eta = S \cdot \frac{k}{\varepsilon}$, $\frac{\eta}{\eta_0} \approx 4.38$, $\zeta = 0.012$, and $C_\mu = 0.085$

Boundary conditions

At high flow velocities, the solid might be dispersed uniformly in the fluid. In this work, the assumption of non-slip boundary condition was imposed for the walls and the transfer of heat has only been considered for parts of the computation domain. Furthermore, near the wall zone the standard wall function has been imposed, as has been proposed by Launder and Spalding^[13]. For $y^* \ll 11.225$ at the wall-adjacent cells, the viscous forces are dominant in the sublayer, hence:

$$u^* = y^* \quad (13)$$

$$y^* = \frac{\rho_m C_\mu^{\frac{1}{4}} k^{\frac{1}{2}} y_p}{\mu_m} \quad (14)$$

The logarithmic law for the mean velocity is known to be valid for $y^* > 11.225$ and is expressed as^[16]:

$$u^* = \frac{1}{k} \ln(E y^*) \quad (15)$$

Where k is von Karman's constant, C_μ is turbulent model constant, k_p and y_p are the turbulent kinetic energy at point p and the distance from point p to the wall, respectively.

As a simplified assumption, the mean velocity inlet and pressure outlet boundary conditions are imposed on the inlet and the outlet of the pipe and are as follows:

$u_{x,\text{inlet}} = \text{constant}$, $u_{y,\text{inlet}} = u_{z,\text{inlet}} = 0$, and $p_{\text{outlet}} = \text{constant}$ (16)

In this work, the turbulence intensity level (i.e., I) was set as 1% for the average velocities.

NUMERICAL COMPUTATION

Physical problems and grid system

In this work, the geometry and physical problems are as follows: length of horizontal straight pipeline (i.e., L) was 1.5 meter; inner diameter of the horizontal straight pipe (i.e., d) was 0.0225 meter; range of the volume fraction of solids (i.e., α_k) was 20%; range of mean velocities of the slurry flow was 1-2 m/s; the density of

Full Paper

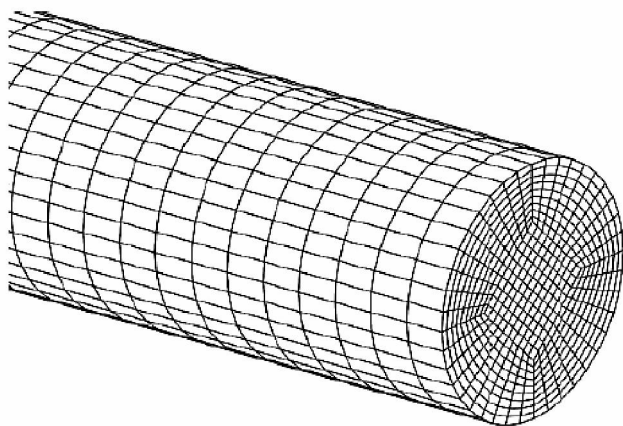


Figure 1: Unstructured grid for the solid–liquid flow pipeline

water was 998.2 kg/m³; the density of silica sand was 2381 kg/m³; mean particle diameter (i.e., d_p) was 0.00011 meter and water temperature was 20 °C.

The length of the computation domain (i.e., x/d 50) was used as the entrance region of the solid-liquid flow, and $x/d > 50$ as fully developed turbulent flow region, as was suggested by Wasp and Brown^[17,18]. A multi-block unstructured, non-uniform grid system with hexahedral elements was used to discretize the computation domain, as shown in Figure 1. The unstructured grid system had five blocks to form the entire computation domain. The distribution of the grid on the circumference of the computation domain was uniform. As a contrast to the fully developed region, finer grid was utilised in the region close to the inlet. The first near-wall cell was placed in such a way that its y^+ value was close to 30.

The grid independency test for obtaining the optimum grid (i.e., 825*9000) is shown in

Table 1 : Grid independent test ($V = 2$ m/s, $a_k = 0.2$, $d_p = 0.00011$ m, silica sand–water slurry flow)

Cross-sectional _ axial	700*8500	750*9000	825*9000	850*9000	900*9000
Total cells	595000	6750000	7425000	7650000	8100000
Dp/DL (Pa/m)	984	1000	1136	1128	1140

discrete governing equation was linearized implicitly with respect to the equation's dependent variable. A point implicit (Gauss-Seidel) linear equation solver was utilised in conjunction with an algebraic multi-grid (AMG) method to solve the resultant scalar system of equations for the dependent variable in each cell. The numerical computation was considered converged when the residual summed over all the computational nodes at n th iteration (i.e.,) was satisfied with the following criterion:

$$\frac{R_{\phi}^n}{R_{\phi}^m} \leq 10^{-4} \quad (17)$$

where is the maximum residual value of ϕ variable after m iterations.

RESULTS AND DISCUSSION

Validation test

The mean pressure gradient in the solid-liquid flow is one of the key parameters in the slurry transportation

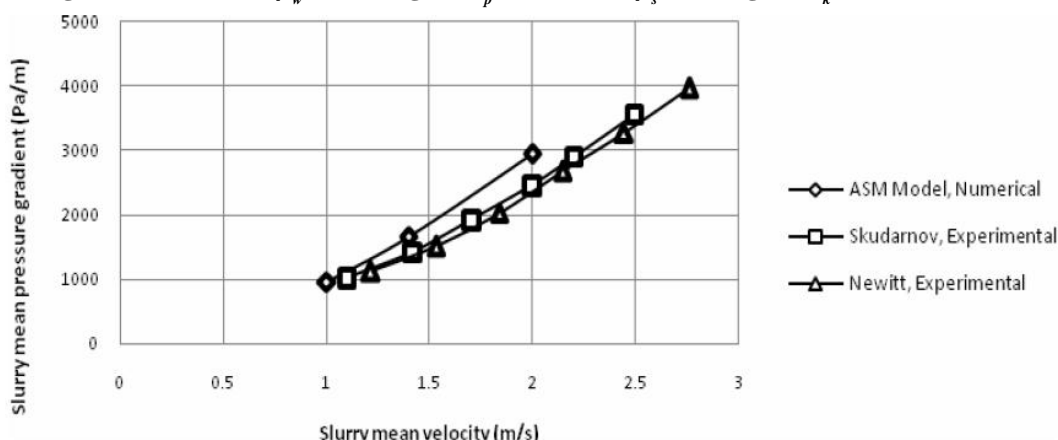
Table 1. Since three-dimensional multi-block was utilised in this work; hence, unstructured grid system adopted. In this work, V was the mean velocity of the solid-liquid flow and Dp/DL was the mean pressure gradient. As

Table 1 demonstrates, when the grid refines an increase in the pressure drop was observed. This shows that the pressure gradient was sensitive to grid change.

Numerical method

In this work, the governing equations, wall boundary conditions and inlet and outlet boundary conditions were solved in a cartesian coordinate system with a CFD commercial code, namely FLUENT. Furthermore, heat transfer was neglected and steady state conditions were assumed. Moreover, the slurry flow were either assumed pseudohomogeneous, heterogeneous flow or heterogeneous and sliding bed flow; depends on the mean flow velocity. The second-order upwind scheme was adopted in this work for the discretization scheme and the convection terms and the central difference was applied in the diffusion terms in the governing equations. The SIMPLE algorithm was adopted to resolve the coupling between the velocity and pressure, as was suggested by Doormaal and Raithby^[19]. To prevent the results to diverge, the under-relaxation technique was applied in all dependent variables. In this work, the under-relation factor for the pressure was 0.2-0.3, for the velocity components was 0.5-0.7 and those for the turbulence kinetic energy and turbulence dissipation rate were 0.6-0.8. The segregated solver was adopted to solve the governing equations sequentially where each

Figure 2 : Comparative studies between the findings of the present study with the experimental data for fully developed turbulent flow region ($d = 0.0225$ m, $\rho_w = 998.2$ kg/m³, $d_p = 0.00011$ m, $\rho_s = 2381$ kg/m³, $\alpha_k = 20\%$).



and pipeline design. As there was no published data available on benchmarking, comparative studies has been made between the experimental data^[20,21] and the findings of the present study using algebraic slip mixture model, as shown in Figure 2:

As Figure 2 demonstrates, the mean pressure gradients from the ASM model are compared with the available experimental data^[20,21] in a single-species slurry flow for the same pipeline geometry, volume fraction of solid particles, particle size and particle density. Figure 2 reveals that there there exist a good compatibility between the findings of the present study and the experimental data and with a discrepancy of as high as 10-15%.

Mean density and volume fraction of solids

For the analysis of solid-liquid flow for the entrance turbulent region, the mean density and volume fraction distributions are of main concern. In practice, it is difficult to measure the mean density and volume fraction of the solid-liquid flow at any point of the entrance region; however, it is easy to obtain these values numerically.

Figure 3 shows the mean density distribution isograms of the silica sand–water flow in the turbulent entrance with $V = 2$ m/s, $\alpha_k = 20\%$, $\rho_s = 2381$ kg/m³, $\rho_w = 998$ kg/m³, $d = 0.0225$ m and $d_p = 0.00011$ m. As Figure 3a demonstrates, relatively small variation of the mean density distribution isograms at the $x/d=15$ are observed. The mean density of the solid-liquid flow usually ranges from 1271 kg/m³ to 1337 kg/m³. As dimensionless length (i.e., x/d) increases, the mean density distribution on the upper section of the pipe decreases; however, a gradual increase in the bottom section are observed. It is worth mentioning that in the central region of the solid-liquid flow, the mean density that ranges from 1271 kg/m³ to 1337 kg/m³ would decrease with an increase of the dimensionless length (i.e., x/d), as shown in Figures 3b and c. Figure 3d demonstrates, the mean density distribution isograms remains constant as the solid-liquid flow reaches a fully developed turbulent flow region. On the upper section of pipe, the mean density of the solid-liquid flow approaches the water density (i.e., 998.2 kg/m³); on the other hand, in the bottom section it would be close to the silica sand density (i.e., 2381 kg/m³). Furthermore, the porosity

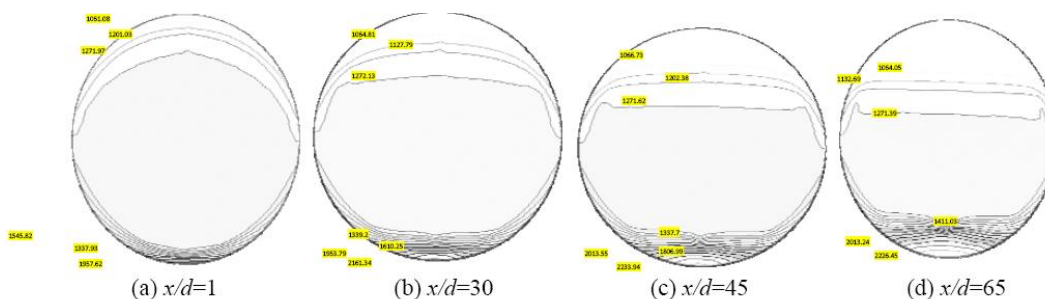


Figure 3 : Mean density distributions of the single-species slurry flow for the entrance of the fully developed turbulent flow region ($\rho_s = 2381$ kg/m³, $\rho_w = 998.2$ kg/m³, $\alpha_k = 20\%$, $d = 0.0225$ m, $d_p = 110$ μ m and $V = 2$ m/s).

Full Paper

distribution in the lower section of the pipe could be characterized by the sand's volume fraction distribution where the porosity are found to be 0.31 in the lower section of the pipe. As Figure 3 demonstrates the distribution of density mixture in the pipe, it was expected that the porosity of the sands accumulated near the bottom of the pipe should drop sharply. However, it occurs only in a very thin layer. It was also concluded that the maximum sediment density or bulk density would reach only near the bottom thin layer section. Furthermore, Figure 3 also demonstrates that the mean density distribution isograms are symmetric in the horizontal direction; however, they are asymmetric in the vertical direction. The mean density of the solid-liquid flow in the upper section of the pipe is much smaller than that in the lower section, due to the solid particles' settlement.

Figure 4 shows the volume fraction isograms of silica sand in the turbulent entrance with $V = 2$ m/s, $\alpha_k = 20\%$, $\rho_s = 2381$ kg/m³, $\rho_w = 998$ kg/m³, $d = 0.0225$ m and $d_p = 110$ μ m. As Figure 4a demonstrates, the volume fraction in the central region ranges from 0.197862 to 0.243189 which is relatively large. Furthermore, in the upper section of pipe the volume fraction was relatively small (i.e., 0.03448) at $x/d = 15$. However, as the dimensionless length (i.e., x/d) increases in the central section, the volume fraction which ranges from 0.197862 to 0.243189 would shrink. Hence, the volume fraction would gradually be increased to 0.04918 in the upper part of the pipe. As Figure 4b and c demonstrates, in the lower section of the pipe the volume fraction was higher than 0.243189, indicating the accumulating of the solids' settlement.

As in Figure 4d shows for the fully developed turbulent flow region, the volume fraction isograms of silica sand would remain constant. However, for upper section of the pipe the volume fraction of silica sand ap-

proaches zero. Similar to the density distribution of the solid-liquid flow, the volume fraction isograms of solids in the horizontal direction was symmetric. However, a gradual increase was observed for the top section of the pipe compared to the bottom section in the vertical direction (Figure 4).

Velocity profiles

The velocity profile of the solid-liquid flow along the horizontal pipeline are mainly affected by the volume fraction of solids, mean density, mean velocity and viscosity of the solid-liquid flow. Therefore, the velocity profile of the solid-liquid flow along the horizontal pipe is not much different from that of single-phase flow. Generally speaking, the velocity profile in the single-phase flow is symmetric and liquid density remains constant in the cross-sectional area of the pipe. However, since the density of solid particles is usually higher than that of liquid, the mean density and the volume fraction of the solid particles in the lower section of the pipe are higher than those in the upper part. In the higher density region (i.e., $\rho_s = 2381$ kg/m³). It demonstrates that a mean velocity of 2 m/s is exerted at the pipe inlet. For the entrance region, the velocity profiles near the wall are reduced sharply due to the strong viscous shear stress in the turbulent boundary layer and non-slip boundary condition on the wall. As shown in Figure 5b-d demonstrates and in order to satisfy the flow continuity equation, the velocity in the central part of the pipe should be increased and the velocity profile of the solid-liquid flow keeps developing in the entrance. In fully developed turbulent flow region, the velocity profiles along the vertical centerline would remain constant. Since the density and viscosity distributions of the solid-liquid flow are asymmetric in the vertical direction, it could be concluded that the velocity profiles of the solid-liquid flow in the upper section of the pipe would be higher than those in the

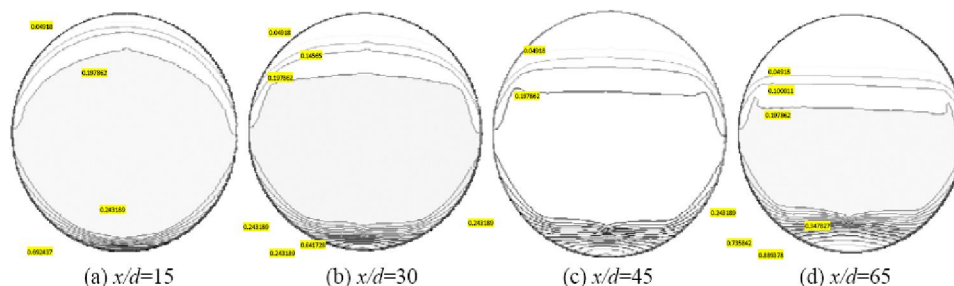


Figure 4 : Volume fraction distributions of silica sand for the entrance of fully developed turbulent flow region ($\rho_s = 2381$ kg/m³, $\rho_w = 988.2$ kg/m³, $\alpha_k = 20\%$, $d = 0.0225$ m, $d_p = 110$ μ m and $V = 2$ m/s).

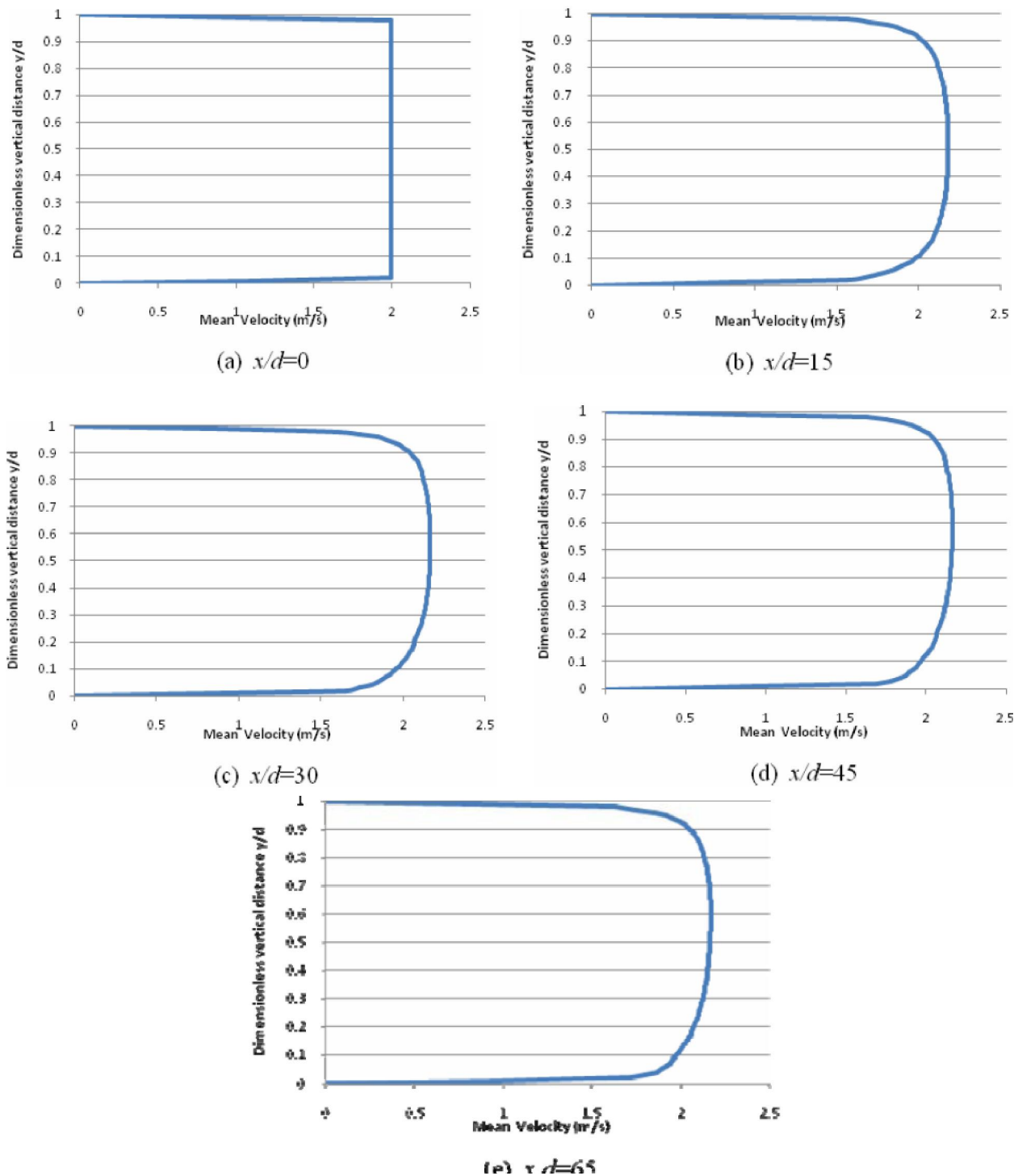


Figure 5 : Velocity profiles of the single-species slurry flows along the vertical centerline for the entrance of fully developed turbulent flow region ($\alpha_k = 20\%$, $d_p = 100 \mu\text{m}$, $\rho_s = 2381 \text{ kg/m}^3$, $\rho_w = 988.2 \text{ kg/m}^3$ and $d = 0.0225 \text{ m}$).

lower part (Figure 5e). Furthermore, the maximum velocity in the center would move up gradually along the vertical centerline of the pipe in comparison with the single-phase flow where a maximum velocity was observed in the centerline. Therefore, as shown in Figs. 5b-e the velocity distribution in the fully developed tur-

bulent flow region was asymmetric in the vertical direction.

Figure 6 demonstrates the velocity isograms of single-species slurry flow (silica sand-water slurry) for the entrance region of fully developed turbulent flow region. Similar to

Full Paper

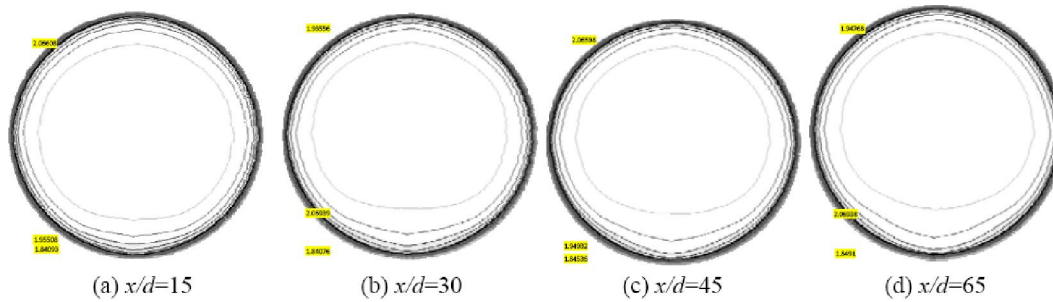


Figure 6 : Velocity isograms of single-species slurry for the entrance of fully developed turbulent flow region ($\rho_s = 2381 \text{ kg/m}^3$, $\rho_w = 988.2 \text{ kg/m}^3$, $\alpha_k = 20\%$, $d = 0.0221 \text{ m}$, $d_p = 110 \text{ }\mu\text{m}$ and $V = 2 \text{ m/s}$).

Figure 5, the location of maximum velocity of the solid-liquid $\hat{u}ow$ would gradually enhances from the entrance region and would remains constant at the end for the fully developed turbulent $\hat{u}ow$ region. Since the density, volume fraction and $\hat{u}ow$ resistance of the solid-liquid $\hat{u}ow$ along the vertical centerline are symmetric in the horizontal direction, Figure 6 also demonstrates that the velocity isograms of solid-liquid $\hat{u}ow$ are symmetric in the horizontal direction.

CONCLUSIONS

It was the aim of this work to determine the volume fraction and velocity isograms in slurry flow (i.e., silica sand-water) in a horizontal pipe using algebraic slip mixture model. The findings of this study could be categorized and the following conclusions could be made:

The algebraic slip mixture model could provide a good prediction for single species slurry $\hat{u}ows$

The findings of this study reveals that the pressure gradients in the single-species slurry $\hat{u}ow$ agrees with a good degree of accuracy with the available experimental data.

For the entrance region, the distributions of mean density and volume fraction of solids would gradually reduce in the upper section of the pipe; however, would increase in the lower section

In fully developed turbulent $\hat{u}ow$ region, the distributions of mean density and volume fraction remains constant

On the top section of the pipe, the mean density of the solid-liquid $\hat{u}ow$ approaches similar to that of primary $\hat{u}uid$ and the volume fraction of solids reaches zero

In comparison with the single-phase $\hat{u}ow$, the location of maximum velocity center in the solid-liquid $\hat{u}ow$

enhances gradually along the vertical centerline in the entrance region

The velocity profiles of solid-liquid $\hat{u}ow$ are asymmetrical in the vertical direction; however, the velocity profiles are symmetric in the horizontal direction.

NOMENCLATURE

	secondary phase particle's acceleration (m/s^2)
C_{1l}	a constant
C_{2l}	a constant
$C\mu$	a constant
d_p	solid particle diameter (m)
E	empirical constant
F	body force (N/m^2)
g	acceleration of gravity (m/s^2)
I	turbulent intensity level
k	turbulent kinetic energy (m^2/s^2)
k_v	von Karman's constant
k_p	turbulent kinetic energy at point p (m^2/s^2)
L	pipeline length (m)
Pr_t	turbulent Prandtl number for energy
S	modulus of the mean rate-of-strain tensor
t	time (s)
u_m	mass-averaged velocity (m/s)
u_{DK}	drift velocity (m/s)
u_p	mean velocity of the $\hat{u}uid$ at point p (m/s)
V	solid-liquid mean velocity (m/s)
	slip velocity (m/s)
X^{qp}	distance along the pipe centerline (m)
y_p	distance from point p to the wall (m)
ΔB	roughness function
$\Delta p/\Delta L$	mean pressure gradient of the solid-liquid $\hat{u}ow$ (Pa/m)
	Greek symbols
α_k	volume fraction of solids

β	coefficient of thermal expansion
ρ	density (kg/m ³)
ε	dissipation rate of turbulent kinetic energy (m ² /s ³)
μ	dynamic viscosity, N s/m ²
τ_{pq}	particulate relaxation time (s)
Subscripts	
i, j, k	general spatial indices
m	mixture
s, w	silica sand and water

ACKNOWLEDGMENTS

The authors wishes to gratefully acknowledge the helpful comments made by Mr. Nezhadhassan in this work.

REFERENCES

- [1] P.Doron, D.Barnea; Flow pattern maps for solid-liquid flow in pipes, *Int.J.Multiphase Flow*, **22**, 273–83 (1996).
- [2] B.R.Thompson, D.Maynes, B.W.Webb; Characterization of the hydrodynamically developing flow in a microtube using MTV.*J.Fluid.Eng.*, **127**, 1003-12 (2005).
- [3] J.Orù, N.Galanis; Mixed convection with heat and mass transfer in horizontal tubes, *Int.Comm. Heat Mass Transfer*, **32**, 511-9 (2005).
- [4] M.A.Al Araby, M.K.Shaban, A.S.Salem, M.M.Mahmoud; Laminar combined free & forced convection heat transfer in the entry length of a horizontal pipe, *Proc ASME Heat Transfer/Fluid Eng.Summer.Conf.*, **1**, 541-51 (2004).
- [5] M.Li, R.I.L.Guthrie; Numerical studies of the motion of particles in current-carrying liquid metals flowing in a circular pipe, *Metall Mater Trans.B.: Process Metall Mater Process Sci.*, **31**, 357-64 (2000).
- [6] J.M.Coldwell, C.A.Shook; Entry length for slurries in horizontal pipeline flows, *Can.J.Chem.Eng.*, **66**, 714-20 (1988).
- [7] J.Ling, C.X.Lin, M.A.Ebadian; Numerical investigation of double-species slurry flow in a straight pipe entrance, *ASME IMECE, Heat transfer Div.*, **372**, 145-54 (2000).
- [8] P.V.Skudarnov, C.X.Lin, M.A.Ebadian; Double-species slurry flow in a horizontal pipeline, *J.Fluids Eng.*, **126**, 125-32 (2004).
- [9] K.K.Jerry; Experimental investigation of spatial concentration spectra of a solid in a slurry in horizontal pipeline flow, *Flow Meas Instrum.*, **5(3)**, 155-63 (1994).
- [10] P.Doron, D.Barnea; A three-layer model for solid-liquid flow in horizontal pipes, *Int.J.Multiphase Flow*, **19**, 1029-43 (1993).
- [11] K.C.Wilson, F.J.Pugh; Dispersive-force modelling of turbulent suspension in heterogeneous slurry flow, *Can.J.Chem.Eng.*, **66**, 721-7 (1988).
- [12] V.Nassehi, A.R.Khan; A numerical method for the determination of slip characteristics between the layers of a two-layer slurry flow, *Int.J.Numer.Method Fluid.*, **14**, 167-73 (1992).
- [13] P.Doron, D.Granica, D.Barnea; Slurry flow in horizontal pipes-experimental and modeling, *Int.J.Multiphase Flow*, **13(4)**, 535-47 (1987).
- [14] M.Manninen, V.Taivassalo, S.Kallio; On the Mixture Model for Multiphase Flow, Technical Research Center of Finland, VIT Publications, (1996).
- [15] B.E.Launder, D.B.Spalding; The numerical computation of turbulent flows.*Comput. Method Appl.Mech.Eng.*, **3**, 269-89 (1974).
- [16] Fluent Inc.FLUENT 5, User's Guide, (1996).
- [17] E.J.Wasp, J.P.Kenny, R.L.Gandhi; Solid-liquid flow: slurry pipeline transportation, Houston, Texas, Gulf Publishing Co., (1979).
- [18] N.P.Brown, N.I.Heywood Slurry handling: design of solid-liquid systems, New York, Elsevier Science Publishing Co., (1991).
- [19] J.Dormaal, G.D.Raithby; Enhancement of the SIMPLE method for predicting incompressible flow problems, *Numer Heat Transfer*, **7**, 147-58 (1984).
- [20] P.V.Skudarnov, H.J.Kang, C.X.Lin, M.A.Ebadian, P.W.Gibbons, F.F.Erian et al.; Experimental investigation of single and double-species slurry transportation in a horizontal pipeline, In, *Proceedings of the ANS 9th international topical meeting on robotics and remote systems*, (2001).
- [21] D.M.Newitt, J.F.Richardson, M.Abbot, R.B.Turtle; Hydraulic conveying of solids in horizontal pipes.*Trans.Instrum. Chem.Eng.*, **33(2)**, 93-113 (1955).